ELSEVIER

Contents lists available at ScienceDirect

## **Quaternary Science Advances**

journal homepage: www.sciencedirect.com/journal/quaternary-science-advances





# GIS-based MCDM approach for landslide hazard zonation mapping in east Gojjam zone, central Ethiopia

Chalachew Tesfa\*, Demeke Sewnet

Debre Markos University, Technology Institute, Debre Markos, Ethiopia

#### ARTICLE INFO

Keywords: GIS AHP Inventory mapping Causative factors Landslides

#### ABSTRACT

Landslides are prevalent in the Ethiopian highlands, particularly in the east Gojjam zone, which is highly affected by landslide problems. This research was carried out in the east Gojjam zone, northwestern Ethiopia. The study area is part of an economically important area in the country, and it is the main source of water for the Grand Ethiopian Renaissance Dam (GERD). The main objective of this work was to undertake a detailed inventory of past landslide locations and prediction of present and future landslide hazards, as well as the preparation of a landslide zonation map in the East Gojjam zone by using the Analytical Hierarchy Process (AHP) with the GIS technique. The parameters used for this study were slope degree, slope aspect, land use and land cover, road proximity, rainfall, lithology, altitude, and river proximity. The various causative parameters were collected from the field, and suitable modifications were made to the thematic maps. Finally, the ratings for various parameters were used as the basis to prepare the LHZ map in GIS windows. The landslide susceptibility and inventory mapping were produced in the GIS environment. The results of the study show that the main driving factors for the landslide hazards in the area were river proximity, rainfall, and manmade activities. Validation of this LHZ map revealed that more than 80% of past landslides match within the "high hazard zone" and reasonably accepted the rationality of the adopted methodology. The considered parameters, as well as their evaluation of the production of LHZ-Map, were confirmed. The produced landslide inventory map is very important for urban planners, agricultural studies, environmentalists, and future landslide hazardous prevention and mitigation strategies.

#### 1. Introduction

Landslides or slope failures, which are complex natural phenomena with a wide variety of slope movements like falls, slides, spreads, flows, and creep, are serious natural hazards that occur in many countries (Crozier and Glade, 2005; Asmare and Tesfa, 2022; Asmare et al., 2023). Landslide susceptibility is defined as the spatially and temporally independent chance of landslides happening in a given location based on local topographic characteristics (Guzzetti et al., 1999, 2005). Landslide susceptibility maps are based on the idea that landslides will occur under the same conditions as they did in the recent past (Tesfa and Woldearegay, 2021; Addis, 2023). Over 700 landslide sites were recorded in Ethiopia, mostly affecting rural communities where infrastructure, farmlands, dwelling houses, etc. are frequently affected by landslides (Woldearegay, 2013). It is very common to see landslide-related problems along different roads in the country that hinder traffic movements during the rainy season. Groundwater,

uncontrolled surface runoff, joints in rocks, and the presence of a ridge zone within the rocks can be the main causes of slope instability. During the past few years, landslides have damaged road sections and farmlands (Tesfa and Woldearegay, 2021).

Landslide susceptibility can be assessed using a variety of analytical methodologies, including heuristic, statistical, and deterministic methods (Soeters and Van Westen, 1996; Arkar et al., 2023). Statistical landslide hazard assessment has grown in popularity, particularly with the adoption of Geographic Information Systems (GIS) and the ability to use data integration techniques established in other fields (van Westen et al., 2005; Van Westen et al., 2006; Di Napoli et al., 2021; Yang et al., 2023). By using a multi-criteria decision approach (MCDA) with a complete database of historical landslide locations and GIS tools to analyze the primary causative elements and map landslides.

The following criteria were taken into account for this study: slope material (lithology), land use and land cover, rainfall, river proximity, road proximity, and man-made activities. The expert evaluation was

E-mail addresses: chalachew\_tesfa@dmu.edu.et, chalachewtesfa@gmail.com (C. Tesfa), demekeswnt2002@gmail.com (D. Sewnet).

<sup>\*</sup> Corresponding author.



Fig. 1. Some of the observed landslide at Dejen (Bore bor Gobez Amba) area.



Fig. 2. Some of the observed landslide problems in the area (Aba Libanos, Tiba).

used to provide a suitable rating for the different causative parameters (Ermias et al., 2017; Shano et al., 2020). Finally, the ratings for the different characteristics are utilized to generate the LHZ map in GIS windows. The landslide susceptibility influence of the causative factors was calculated in a GIS environment to determine and select the influencing factors that lie inside each landslide area.

Ethiopia faces many disasters, both natural and human-made, which include floods, drought, stormy rains, earthquakes, outbreaks, fire, and accidents. The problem is more pronounced in Amhara Regional State. Many factors, including but not limited to climate change, rapid population growth, a construction boom, economic growth, and the consequent environmental degradation, are increasing the intensity and frequency of disasters. North-West Ethiopia has experienced repeated landslide activities (Tadele, 2022). These landslides are of different types, from shallow soil creeping to huge, deep-seated landslides with appreciable consequences. Some areas of Amhara Regional State that are highly affected by geohazards are located in the East and West Gojjam Administrative Zones, as evidenced by their extreme conditions, including heavy rains that result in floods. In these areas, geohazards are present even at present.

One of the areas in the Amhara regional state that is continuously affected by the geohazard is the east Gojjam zone. The landslides in this zone occurred so many times in different localities like Abalibanos (Tiba area), Lumame, Dejen, Choke, Woyinma Geramo, Debre work, and soon. The nature, severity, impact they brought on lives, and extent of the damage brought about around three kebeles of Dejen District, namely Amarit, Shencha, and Minji (Fig. 1); Bibugn District (digo around the

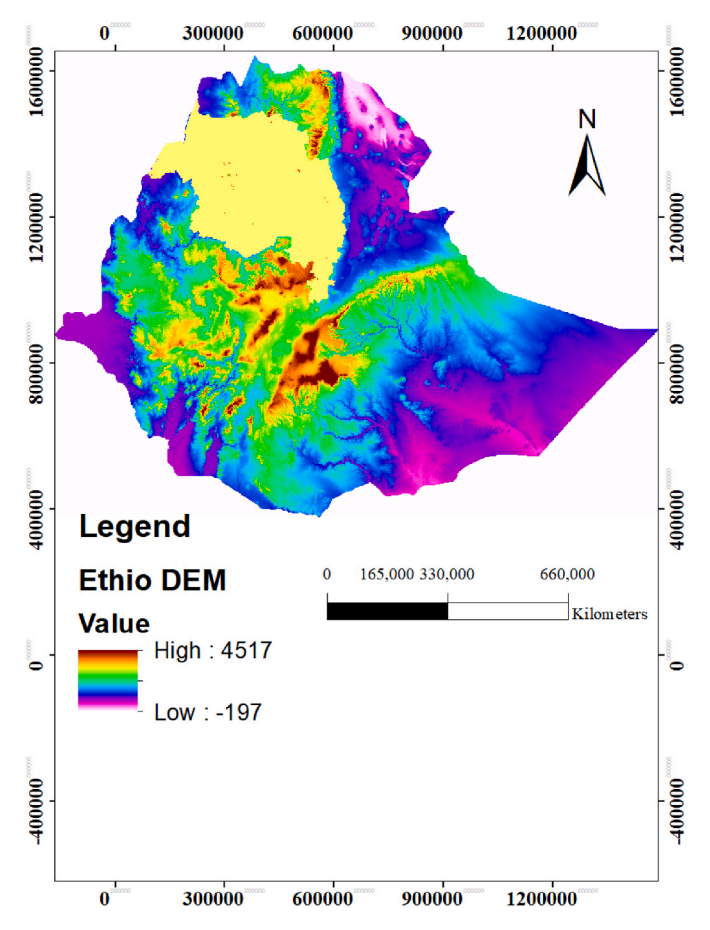


Fig. 3. Location Map of the study area.

hospital); Woyinma Geramo; and one kebele of Awabel District, named Mizan Washa, through social media (TV, Facebook, Telegram, local FM); Districts' communication offices Amhara Mass Media Agency, and calls from friends and directs the community dwellers (Fig. 2).

The study area is part of the economically important areas in the country and the source of water for the Grand Ethiopian Renaissance Dam (GERD). Many rivers and streams are tributaries of the Abbay River. The goal of this work was to map the most susceptible areas for landslides and slope failure. The study was focused on the investigation of geohazard-affected areas, slope-related failure assessment, and landslide hazard zonation mapping in the east Gojjam zone.

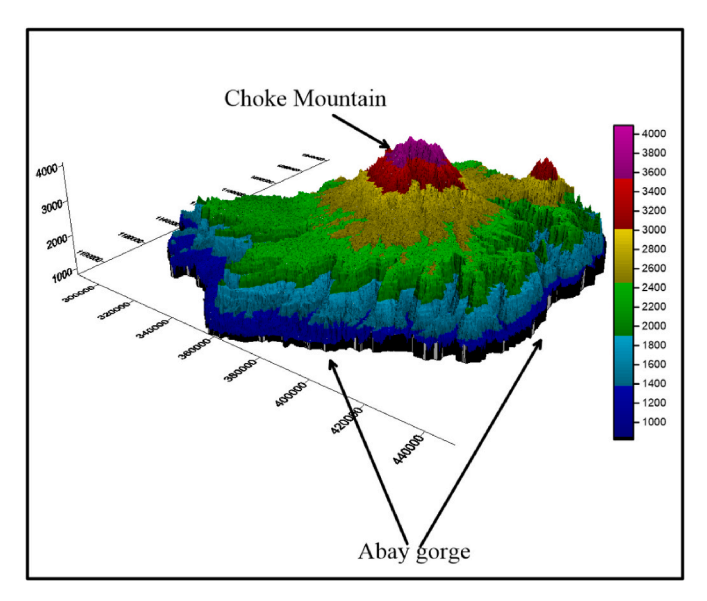


Fig. 4. Physiographic map of the area.

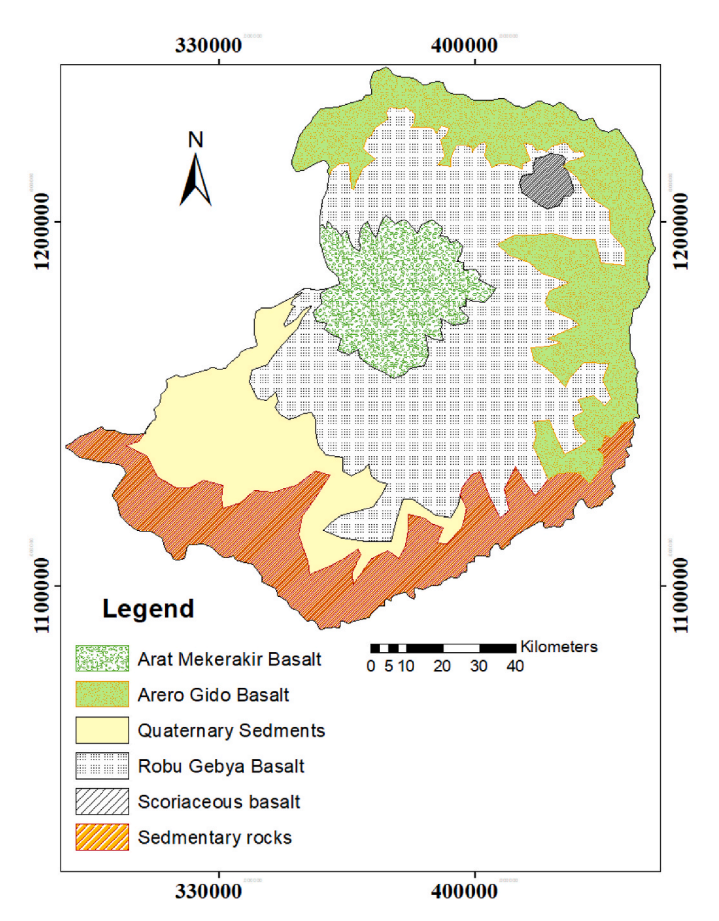


Fig. 5. Geological map of the study area.

#### 2. Descriptions of the study area

#### 2.1. Location

The study area is situated in the East Gojjam Zone administration, Amhara Regional State, in the northwestern part of Ethiopia. Geographically, the study area is described by latitudes of 250000 m-300000 m and longitudes of 1050000 m-1550000 m (Fig. 3). The

study area is accessed by an asphalt road that runs from Addis Ababa (the capital city of Ethiopia) to Bahir Dar, Gondar, and then Sudan by crossing the border, and the study area is found starting from Abbay gorge in this road section.

The east Gojjam zone administration is one of the Amhara regional state administrative areas that is bounded by the west Gojjam zone at the west, Oromia regional state at the south and southeast, as well as the study area, which is bounded as a belt by the Abbay river, with more than half of its territory bounded by the Abbay river.

## 2.2. Physiography and climate

The physiographic setting of the Amhara regional state is a very ragged topography and is mostly characterized by highland areas. One of the highlands and mountainous areas in the study area is Choke Mountain. The area is topographically highly dissected, and its altitude ranges from 818 to 4094 m a.m. s.l. Plane land, mountainous, and conical ridges are the most commonly observed landforms in the area (Fig. 4). The climatic condition of the mountain range is divided into six distinct climate zones, and Choke Mountain's peak, Wurch, is located at 3200 m above sea level in a humid climate with an annual average temperature of fewer than 11.5 °C (Simane et al., 2013). The area received an annual rainfall of 1206 mm and 1596 mm minimum and maximum, respectively (Fig. 8f).

#### 2.3. Geological setting of the area

The geological setting of the study area is characterized by the voluminous tertiary volcanic that cap the Mesozoic sediments, which are exposed only in the deep incisions of major rivers like Abbay, Jemma, and other minor rivers. The Paleozoic-Mesozoic sediments are associated with transgression and regression of the sea and Cenozoic volcanic rocks, which are directly overlying the Precambrian metamorphic and Mesozoic sedimentary rocks in Ethiopia (Kazmin and Garland, 1973). The main litho-stratigraphic units presented in the study area are Mesozoic sedimentary rocks, Cenozoic volcanic rocks, and Quaternary superficial deposits. Sandstone is the main rock unit that belongs to the Mesozoic sedimentary formation. Generally, the geology of the area is characterized as follows:

- Arat Mekerakir Basalt: This unit is exposed to the choke mountain area, locally called the Arat Mekerakir Mountains, which are mostly covered by this type of basaltic rock. Compositionally, the rock shows plagioclase phyric and olivine plagioclase basalts (Fig. 5). The basalt is dark, porphyritic, aphyric, occasionally vesiculated, and amygdaloidal with silica amygdules. It is dated at 22.4 Ma (Kieffer et al., 2004) and exposed towards the top of Choke Mountain, near the Choke Mountain peak. Choke Peak Basalt is the thin layer exposed at the topmost part of Choke Mountain, in the northwestern part of the study area (Fig. 5). It forms a flat-lying area at the topmost part of Choke Mountain.
- Arero Gido Basalt: This unit is exposed in the northeast part of Mertolemariam town. Compositional basalt is expressed as oliven pyric basalt and oliven plagioclase phyric basalt. The top part of this area is covered by volcanic braccia. Occasionally, the pyroclastic tuff is interlayered with this basalt. The topmost part of this unit is occupied by volcanic breccia (basaltic composition) or sandstone at places. The basaltic breccia is dominated by volcanic breccia, with a maximum volcanic block size of 40 cm and a maximum thickness of 50 m in field observation.
- Robu Gebya Basalt: This unit has a variable interval of phenocryst proportion. This unit is exposed at the base of the Choke Mountain series. The Robu Gebya basalt is dark, porphyritic, with occasional aphyric texture, and sometimes vesiculated and amygdaloidal with silica amygdules. It is plagioclase phyric basalt, olivine-plagioclasepyroxene phyric basalt, and pyroxene-olivine phyric basalt.

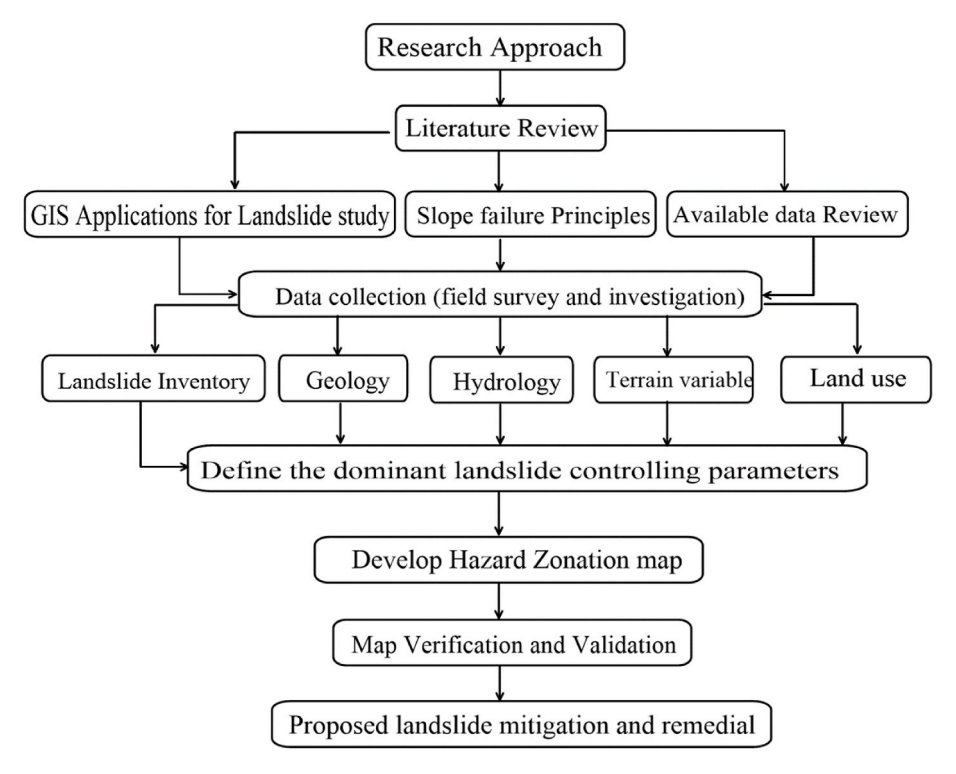


Fig. 6. Flow chart showing the sequence of the study.

**Table 1**Conditioning factors and their respective data sources.

No	Conditioning factors	GIS data type	Scale	Data Source
1	Landslide inventory	Polygon	1:50,000	Field observation GPS point data, Google Earth image (2023)
2	Lithology	Polygon	1:50,000	Geological map of Ethiopia ( Tefera et al., 1996), Field observations
3	Elevation	Grid	30 × 30	DEM Data (30 $\times$ 30 m) ASTER data set
4	Aspect	Grid	$30 \times 30$	DEM Data (30 × 30 m) ASTER data set
5	Slope	Grid	$30\times30$	DEM Data (30 $\times$ 30 m) ASTER data set
6	Land use/cover	Grid	$30\times30$	https://livingatlas.arcgis. com/landcover/
7	Road Density	Polyline	$30 \times 30$	road density of Ethiopia
8	Drainage Density	Grid	$30 \times 30$	DEM Data (30 × 30 m) ASTER data set
9	Rainfall	Grid	$30 \times 30$	https://crudata.uea.ac.uk/cru/data/hrg/cru ts 4.06/

- Scoriaceous Basalt: This unit occurred by covering the Islamo mountain with the formation of scoriaceous basalt and a cone at the top of the mountain. It symbolizes a well-known Islamo mountain made of volcanic ash. The volcanic pile was created by the separation of three large lava flows by basaltic agglomerate and volcanic breccia, respectively (Fig. 5). This unit's topmost portion has a thin layer of scoria and scoriaceous basalt covering it, forming a scoria cone. The scoriaceous basalt is dark, highly vesiculated, and relatively lightweight with respect to the massive basalt and contains minor mantle xenoliths composed of olivine.
- Sedimentary Rocks: This sandstone unit is referred to as the upper sandstone, or Ambaradom Formation (Tefera et al., 1996). This unit is exposed mainly along the banks of the Abbay and Jema Rivers in the study area (Fig. 5). The rocks are laminated and/or bedded, and

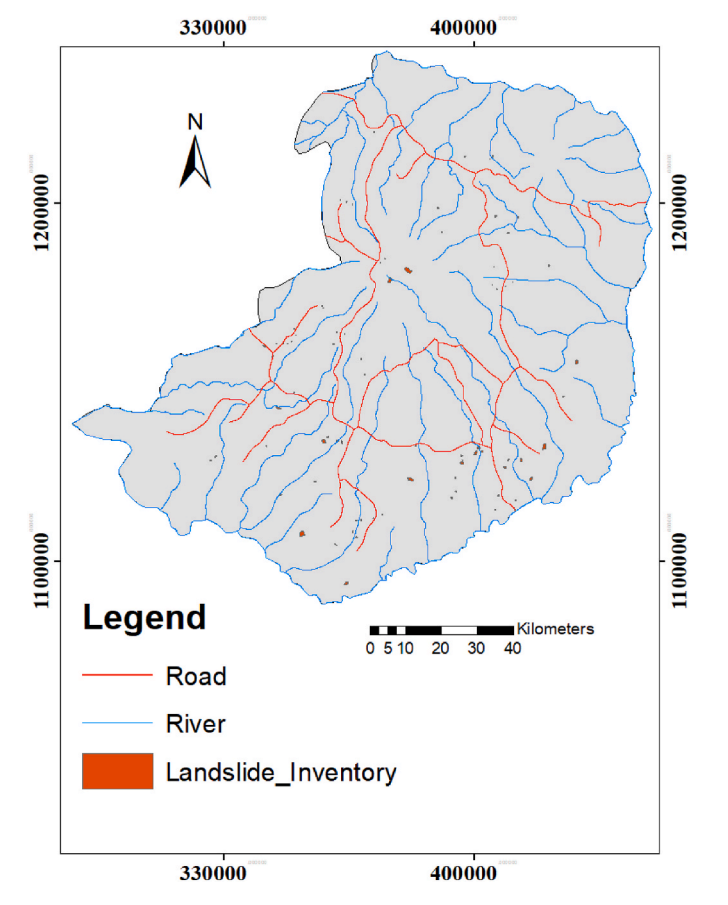


Fig. 7. Landslide Inventory Map of the study area.

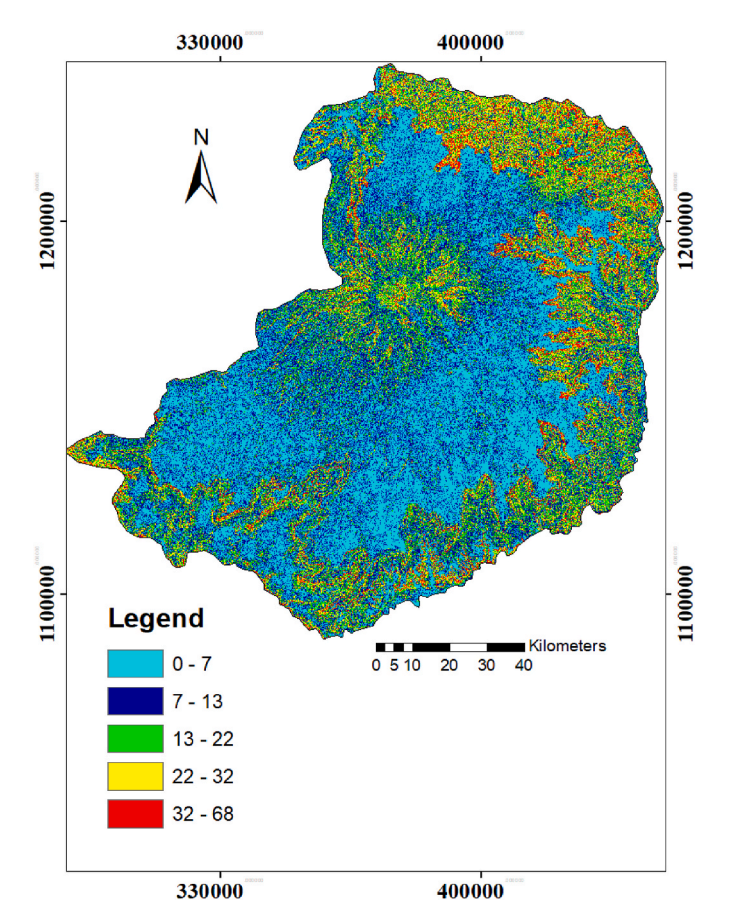


Fig. 8. Slope Degree map of the study area.

the bedding thickness varies from very thinly bedded to thickly bedded. The gypsum conformable to blue shale has a bluish-grey color. The gypsum shows bedding and sometimes develops nodules of fine-grained granular aggregates of the gypsum mineral. The limestone, which alternates with gypsum, is yellow and, bedded thinly and thickly, and occasionally bears fossil fragments. The thin section description for naming limestone is adapted from (Folk, 1959) in this report. The laminations are expressed by fine-grained sand-size layers and silt-size layers, by closely spaced micro-channels, and by channel-infilling clay-sized minerals. The sandstone is light grey, reddish, and bedded.

- Quaternary Sediments: The moderate slope and steep slope to-pographies are susceptible to slope deposits. These sediments occur as a map-able unit north of the Abay River and south of Dejen town in the southern part of the study area (Fig. 5). The slope deposits are friable and vary from massive to locally layered sediments with white tints. The maximum thickness of the slope deposits attained is 5 m. These sediments vary in size and include clay, silt, sand, pebbles, cobbles, and boulders. The boulder was formed from basalt, gypsum, and limestone units.

#### 3. Methodology and approaches

The majority of landslide hazard zones are founded on the fundamental presumption that large-scale movements are due to geological, geomorphological, and human-induced factors. The methodology followed by this study was:

 A detailed field survey of the past landslide-affected areas, GPS records, photography, expert interviewing, lithological records, topographic surveying, hydrogeological conditions, causative

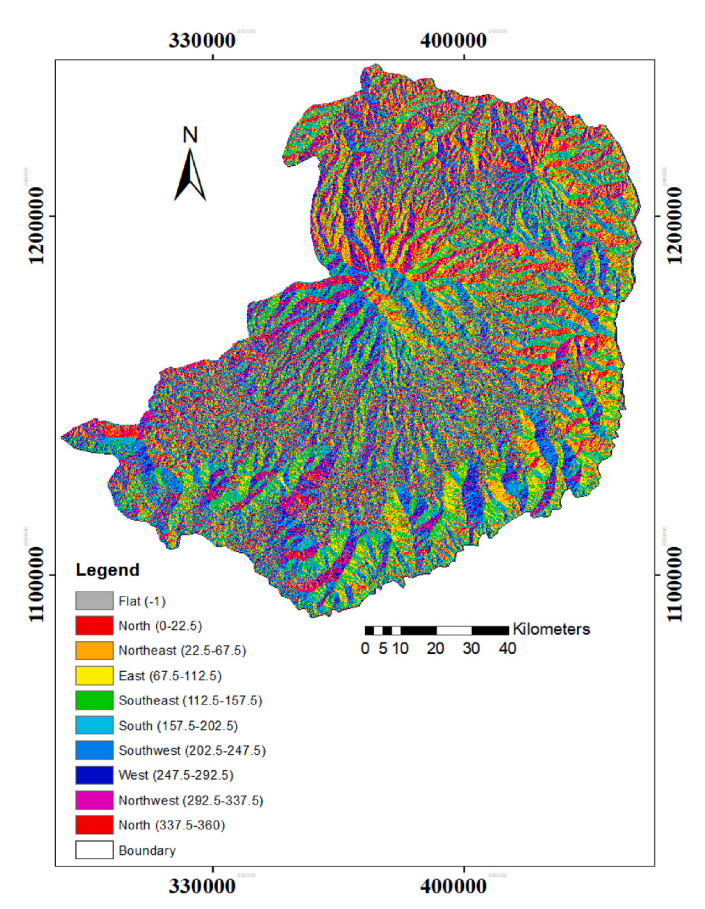


Fig. 9. Slope Aspect Map of the study area.

factor selection, and base map preparation of landslide-affected

- (2) The AHP tool is a multicriteria decision-making method that was originally developed by (Saaty, 2004). It is a method to derive ratio scales from paired comparisons. AHP-based multi-criteria decision-making approach using the selected causative factors in the landslide-affected area was performed to identify the most influencing factor for the occurrence of landslides in the area. Among many alternative multicriteria decision-making tools, the analytical hierarchy process (AHP) was selected for this study as a result; of its wide applicability in landslide susceptibility mapping. The relative importance of each component can be compared to create a pair-wise comparison matrix based on the expert's prior experience and knowledge (Vishwakarma et al., 2021).
- (3) A GIS window was used to map the landslide susceptibility of the study area and prepare of causative factor maps; it was also used for the analysis of susceptibility mapping (Fig. 6).

## 3.1. Data collection

The data for the present study was collected from several sources (Table 1). Primary and secondary data from a variety of sources were obtained for landslide hazard evaluation and mapping techniques (Table 1). The topographical map (1:50,000) was utilized and acquired from the topographic map of the study area. An aerial photograph was also utilized to prepare the slope materials and land use/cover of the area. The input data are prepared and obtained based on a variety of intrinsic and triggering characteristics of the area.

Finally, the sum of all evaluations for all triggering factors resulted in

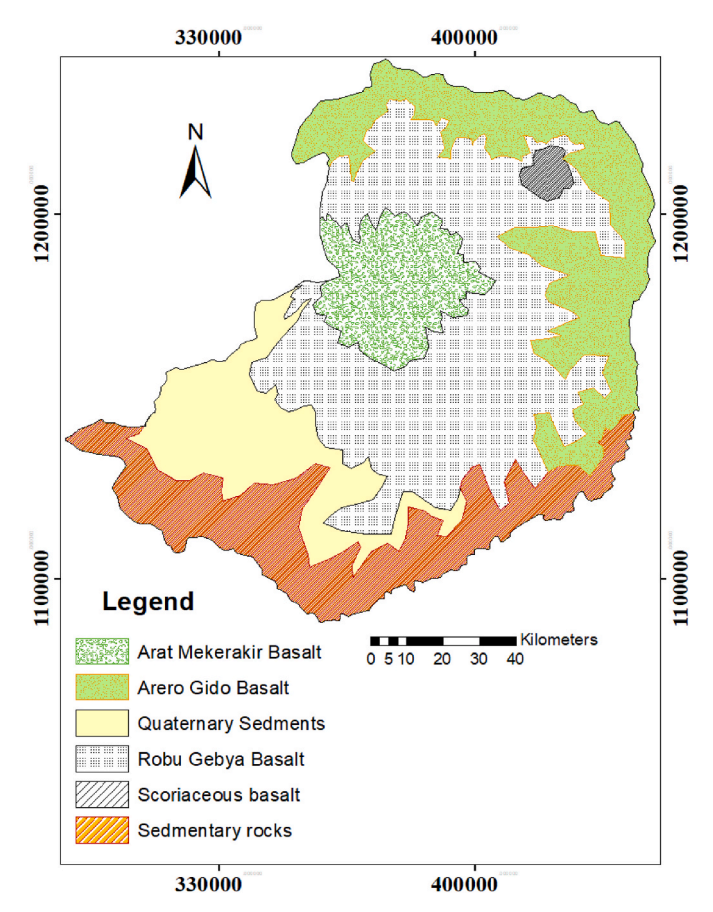


Fig. 10. Geology/Lithology Map of the study area.

an assessment of landslide hazards (ELH), which was used to construct the LHZ map. A landslide inventory map was constructed for this research utilizing field observations, satellite data, and Google Earth photos. The previous landslides that were observed in the region were documented using hand GPS (Fig. 6).

#### 4. Results

## 4.1. Landslide inventory mapping

The inventory mapping of landslides was prepared from the total area covered by landslides and the observed landslide types in the area. This implies that similar landslide scenarios can occur in similar circumstances. Hence, the observed and identified causative factors are detailed investigated, and mapped for further landslide occurrence comparison. A landslide inventory map of the area was prepared based on the following information: a) a field survey using hand GPS; b) Google Earth images c) Literature reviewing and interviewing. Then landslide locations are digitized as polygons by using Arc GIS 10.4 windows (Fig. 7).

## 4.2. Landslide triggering parameters

Most landslide hazards are caused by geological, meteorological, geomorphological, and human-induced factors in general. The landslide causative parameter was selected based on the type of landslide observed and the site area condition ratings as inherent and external triggering characteristics.

The causative factors are described based on the physical parameters, and these conditions enable future landslides (Corominas and Moya, 1999; Lang et al., 1999; Singh et al., 2023). According to

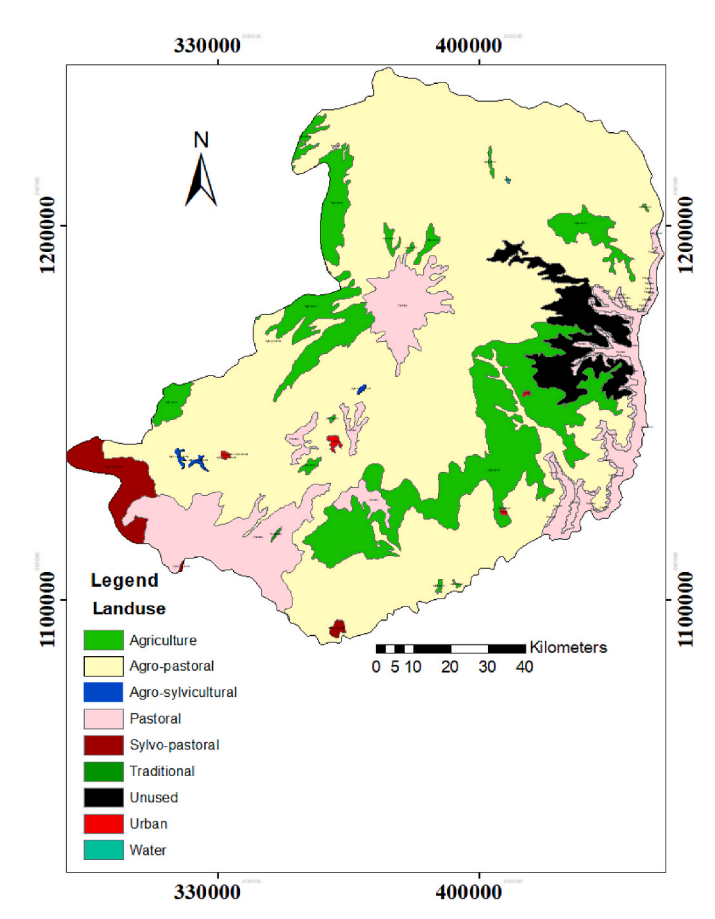


Fig. 11. Land use/Cover Map of the study area.

(Anbalagan, 1992; Qazi et al., 2023), landslide susceptibility maps are prepared using the relationship between each landslide and its causative factors. In the study area, there are rockfalls along the road cut, and several rockfalls are observed in some parts of the area on the cliff sides. The rockfalls mostly seen in the area are on limestone intercalation and basalt units (Abbay gorge areas). Most of the rockfalls were observed as a result of road-cut exposure along the road corridor and river-cut exposure.

Generally, based on the field observation carried out, the primary causes of landslides in the study area are the presence of weathered geological materials, the presence of jointed and fractured rocks, seepage of water into the weathered and cracked layers that are exposed on the surface after the construction of the road, a high gradient and a steep vertical cutting of a slope of 70–85° averagely, and deforestation and land-use changes for agricultural activity.

#### 4.2.1. Slope Degree

The slope degree of the study area was prepared from the DEM using GIS. The slope classes include escarpment or cliff (more than 45°), severe slope (36°–45°), moderately steep slope (26°–35°), mild slope (16°–25°), and very gentle slope (15°). The slope is a vital controlling factor in the area for the landslide susceptibility mapping as a causative factor (Fig. 8).

### 4.2.2. Slope aspect

The aspect map of the study area was also prepared from the DEM of the study area in the GIS environment. Aspect-related parameters such as exposure to sunlight, drying winds, rainfall (wetness or degree of saturation), and discontinuities may control the occurrence of landslides in this factor. The frequencies of landslides are higher in the East, Southeast, Southwest, and West aspect subclass areas (Fig. 9).

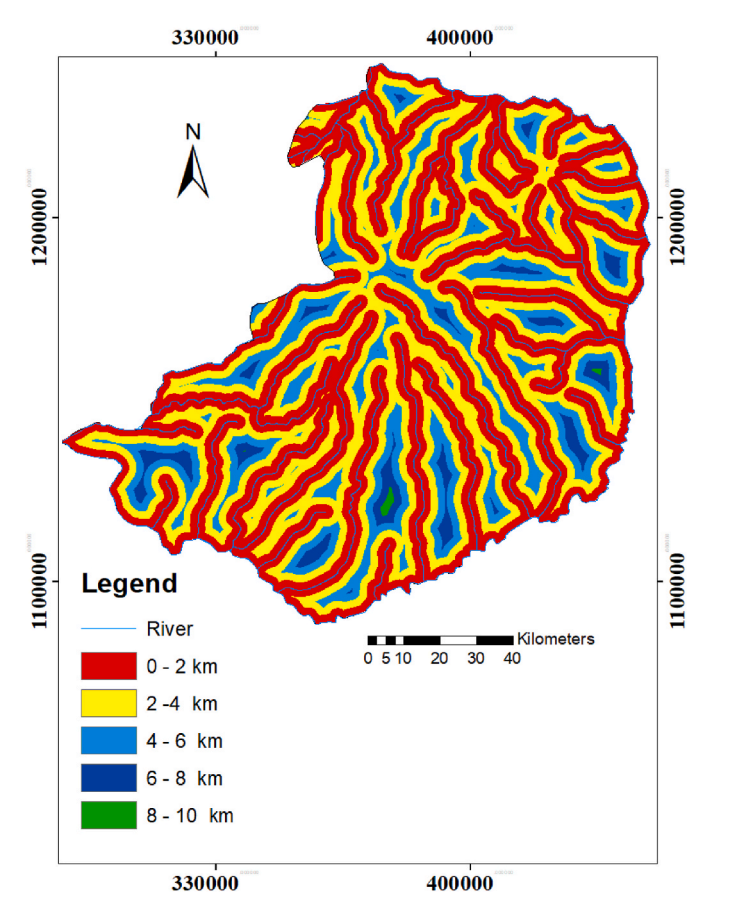


Fig. 12. Distance from the stream map of the study area.

### 4.2.3. Geology/lithology

The lithology of the study area is characterized by highly weathered and disintegrated rock masses that make it difficult to distinguish some rocks from others at some places during the field visit. It found that geologic boundaries often relate to rock strength. A high density of geologic boundaries means lower stability and may lead to an increase in landslide occurrences. Therefore, the distance to geological boundaries is also considered a factor in this study. Six types of lithological units cover the lithology of the study area (Fig. 10).

## 4.2.4. Land use land cover

Slope stability is heavily influenced by land use and land cover patterns. Vegetation has an important role in resisting the slope, especially for failures with shallow rupture surfaces. Because of the inherent anchoring of slope materials, a well-spread network of root systems enhances the shearing strength of the slope material, particularly for soil slopes. Slope instability is also caused by man-made activity, such as urbanization, especially on steeper slopes (>30°). It not only eliminates vegetative cover but also adds to the natural weight of the slope as a surcharge from the weight of civil construction. Buildings are often built on a hill slope with a larger slope angle by creating local cut slopes and flat terraces due to a shortage of land for settlement. It was found at https://livingatlas.arcgis.com/landcover/to do the land use land cover map of the study area. The dominant area is covered by grassland, followed by cultivated land, and the frequencies of landslides commonly observed in the grassland class are according to AHP (Fig. 11).

#### 4.2.5. Distance from the stream

The geological materials on the sides of rivers are affected by water scouring and lateral erosion. The closer the river, the higher the degree of soil erosion and the poorer the stability of the rock bodies (Li et al.,

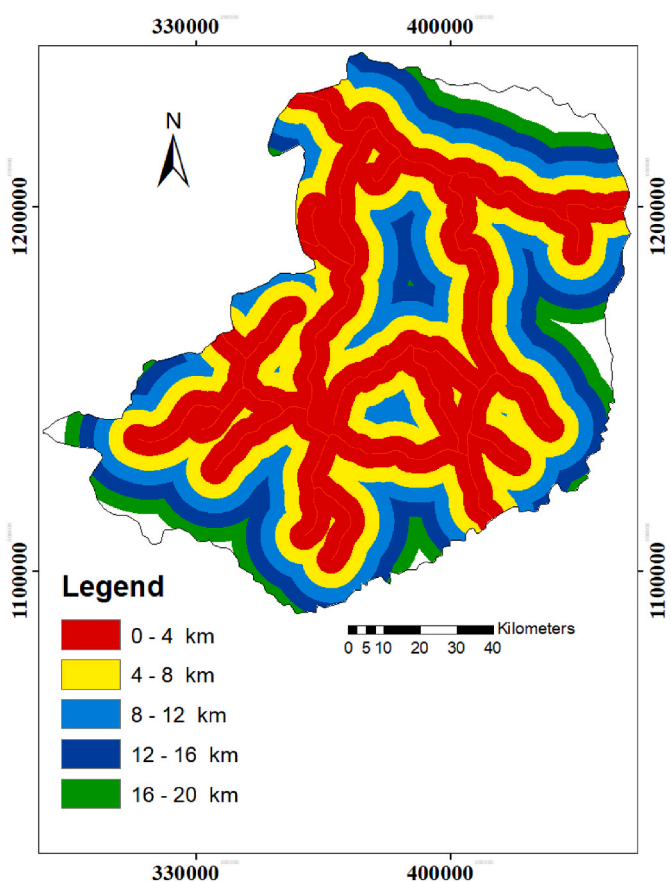


Fig. 13. Distance from the Road map of the study area.

2023). The groundwater of an area plays a vital role in determining the susceptibility of rocks and soil to failure. The hydrological properties of an area include the presence of streams and rivers, underground water conditions, the saturation state of rock and soil, and the drainage pattern of the area. Dislocated water bodies due to the presence of discontinuities and shallow water-table conditions in hilly terrains, along with heavy rainfall, make the slopes prone to instability. According to (Tadele, 2022), during the prolonged monsoon phases, increased pore-water pressure creates favorable conditions for deep-seated land-slide occurrence. A stream distance map was prepared from the drainage pattern map of the area using a 100-m buffer zone in a GIS window (Fig. 12).

## 4.2.6. Distance from the road

The road construction activity and networks disturb the original topography and destroy the rock structure. Particularly in hilly and gully areas, the closer the road is, the more likely it is to induce geological disasters such as landslides and collapses (Tesfa and Woldearegay, 2021; Tesfa, 2022; Zewdie and Tesfa, 2023). In the study area, most, frequent landslides observed on the sides of the road cut exposures occurred consecutively; this means that the road cut may be unstable or the road vibrations by vehicles induced landslides in the area. The landslide frequency is very high in the 1 km buffer zone from the road when compared with 6 km far from the road (Fig. 13).

#### 4.2.7. Altitude/elevation

The altitude map of the study area was prepared from the DEM map of the study area and classified into five different classes: 818–1511, 1511–1954, 1954–2347, 2347–2896, and 2396–4094 m above mean sea level (Fig. 14). The maximum area of the study area is covered by an altitude/elevation of 2347–2896 and the minimum areal coverage of the

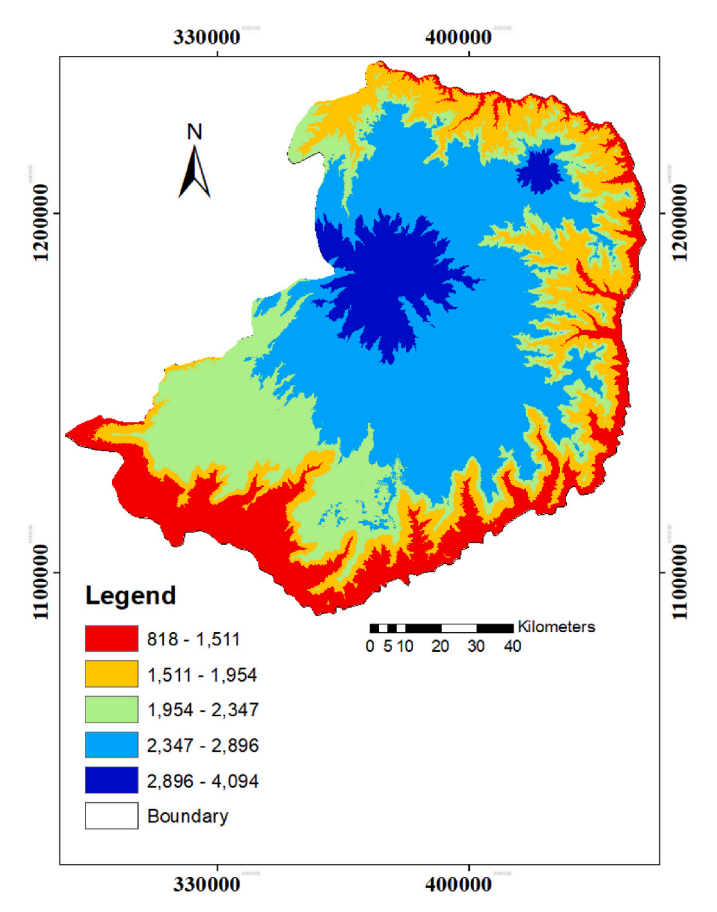


Fig. 14. Altitude/Elevation map of the study area.

study area is covered by 2896-4094m above sea levels.

## 4.2.8. Rainfall/precipitation

Rainfall is crucial to the vegetation ecosystem. However, heavy rainfall in the summer and autumn seasons in the East Gojjam zone exacerbates the degree of soil erosion in loess hilly areas and may induce collapses and landslides. The precipitation data were obtained from htt ps://crudata.uea.ac.uk/cru/data/hrg/cru\_ts\_4.06/for ten years of rainfall from 2011 to 2020 in the east Gojjam zone area. Precipitation is the initiation factor for landslide occurrence due to its significant influence on run-off and water pressure. In this study area, the average monthly rainfall data was collected from ten existing weather stations from the past (Fig. 15).

#### 4.3. AHP analysis of selected causative factors

For this study, evaluations of causative factors related to the occurrence of landslides in the area were based on expert judgments (Table 2). The AHP pairwise comparison of each pair of parameters is carried out by personal judgment. The results of the comparisons are in the form of a matrix. The sum of each column is written below the column. In the next step, the value of each cell is divided by the sum of the corresponding column and written in another table. Then the average of each row is considered the final weight of the related parameter.

The acceptable CR range varies according to the size of the matrix, i. e., 0.05 for a 3 by 3 matrix, 0.08 for a 4 by 4 matrix, and 0.1 for all larger matrices,  $n\geq 5.$  The principal eigenvalue can be calculated from the sum of the products between each element of the eigenvector and the sum of the columns of the reciprocal matrix. All the consistency ratio (CR) values of causative factors show less than 0.1; thus, the matrixes satisfy the consistency requirement.

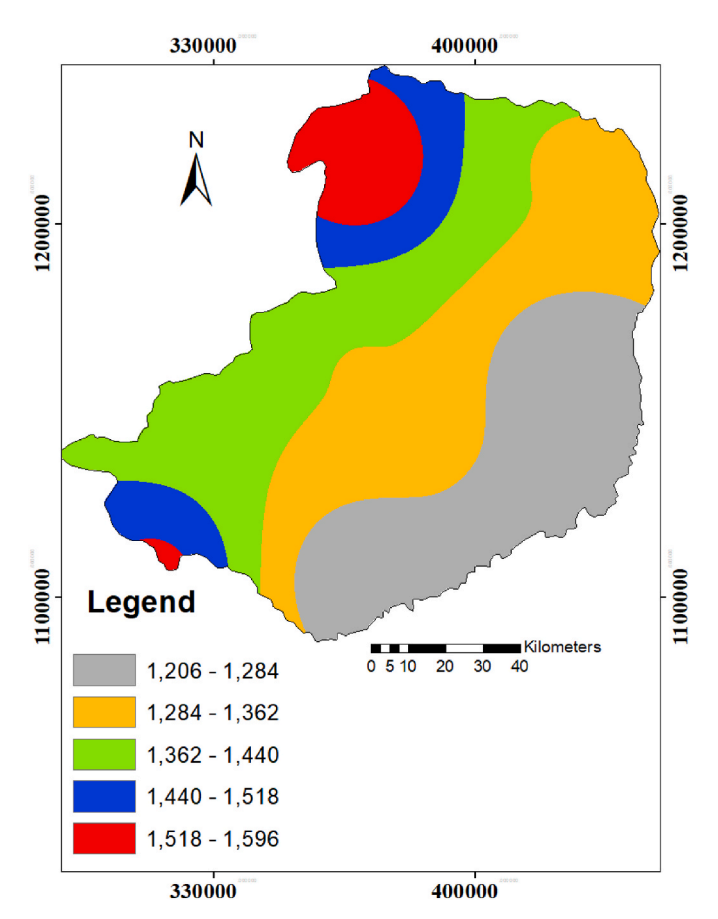


Fig. 15. Map showing rainfall/Precipitation of the study area.

The weights of all factors were determined using AHP-based, topographic, atmospheric, geomorphologic, previous landslide locations, and geologic characteristics judgments. The weight value provides the relative importance of each factor among other factors. Finally, check the consistency of the expert judgments by calculating CI values (Table 3) using Equation (1) below.

$$CI = (\lambda max - n)/(n-1)$$
 (1)

And also we follow (equations: 2) blow to compare it with the random consistency index (RI). Finally, the consistency ratio is calculated by using equations blow.

$$CR = CI/RI$$
 (2)

After parkways comparison matrices are generated for all causative factors, for the preparation of a landslide susceptibility map, landslide susceptibility indexes (LSI) are calculated by using (Equation: 3).

$$LSI = \sum_{i=1}^{n} (Wj * Wij)$$
 (3)

After all this, the produced LSI map was classified into five classes: very low, low, moderate, high, and very high susceptibility. The produced landslide susceptibility map is classified into four susceptibility regions low, moderate, high, and very high (Fig. 16).

## 4.4. Landslide susceptibility mapping

Each controlling factor's weight was assigned using the AHP approach. More effects on the likelihood of landslides could be anticipated as the weight increases. According to Table 2, the weight of the slope was highest, indicating that the slope had the greatest influence on the occurrence of landslides, while the weights of the aspects were

 Table: 2

 Pair-wise comparison matrixes of landslide causative factors.

Sub-Class	[1]	[2]	[3]	[4]	[5]	[6]	[7]	[8]	[9]	Value
Road proximity (km)										
[1] 0-4	1	2	4	5	6	7				0.39
[2] 4–8		1	3	4	5	6				0.27
[3] 8–12			1	3	4	5				0.16
[4] 12–16				1	3	4				0.10
[5] 16–20					1	2				0.05
[6] >20						1				0.04
Geology	[1]	[2]	[3]	[4]	[5]	[6]	[7]	[8]	[9]	Value
[1] Sedimentary Rocks	1	3	4	6	7	9				0.44
[2] Scoriaceous basalt		1	3	4	6	7				0.25
[3] Quaternary Sediments			1	3	5	5				0.15
[4] Robu Gebya Basalt				1	2	3				0.07
[5] Arero Gido Basalt					1	2				0.05
[6] Arat Mekerakir Basalt						1				0.03
Degree of Slope	[1]	[2]	[3]	[4]	[5]	[6]	[7]	[8]	[9]	Value
[1] 32–68	1	2	4	5	6					0.43
[2] 22–32		1	3	4	5					0.28
[3] 13–22			1	3	4					0.15
[4] 7–13				1	2					0.08
[5] 0–7					1					0.05
Aspect Slope	[1]	[2]	[3]	[4]	[5]	[6]	[7]	[8]	[9]	Value
[1] North	1	2	2	3	4	5	6	7		0.30
[2] Northeast		1	1.5	2	3	4	5	6		0.21
[3] East			1	1.5	2	3	4	5		0.16
[4] Southeast				1	1.5	2	3	4		0.11
[5] South					1	2	2	3		0.08
[6] Southwest						1	2	3		0.06
[7] West							1	2		0.04
[8] Northwest								1		0.03
Stream proximity (km)	[1]	[2]	[3]	[4]	[5]	[6]	[7]	[8]	[9]	Value
[1] 0–2	1	2	4	5	7	8				0.40
[2] 2–4		1	3	4	6	7				0.28
[3] 4–6			1	3	5	5				0.16
[4] 6–8				1	2	3				0.08
[5] 8–10					1	2				0.05
[6] >10						1				0.03
Elevation (m)	[1]	[2]	[3]	[4]	[5]	[6]	[7]	[8]	[9]	Value
[1] 818–1511	1	2	3	4	5					0.41
[2] 1511–1954		1	2	3	5					0.27
[3] 1954–2347			1	2	3					0.16
[4] 2347–2896				1	2					0.10
[5] 2896–4094					1					0.06
Land use & Cover	[1]	[2]	[3]	[4]	[5]	[6]	[7]	[8]	[9]	Value
[1] Agriculture	1	2	3	4	6	6	7	8	9	0.31
[2] Agro - pastoral		1	2	3	4	5	6	7	8	0.22
[3] Agro - sylvicultural			1	2	3	4	5	6	7	0.15
[4] Pastoral				1	2	3	4	5	6	0.11
[5] Sylvo - pastoral					1	2	3	4	5	0.08
[6] Traditional						1	2	3	4	0.05
[7] Unused							1	3	3	0.04
[8] Urban								1	2	0.03
[9] Water									1	0.02
Rainfall (mm)	[1]	[2]	[3]	[4]	[5]	[6]	[7]	[8]	[9]	Value
[1] 1206–1284	1	3	4	6	7					0.48
[2] 1284–1362		1	3	4	5					0.25
[3] 1362–1440			1	3	4					0.15
[4] 1440–1518				1	2					0.07
[5] 1518–1596					1					0.05

Table: 3 Causative factors priority Par ways Comparison factor weight,  $\lambda$  max, CI and CR.

Factors	[1]	[2]	[3]	[4]	[5]	[6]	[7]	[8]	Weight
[1] Rainfall	1	1.5	2	3	4	6	6	7	0.26
[2] Lithology		1	2	3	4	5	6	7	0.24
[3] Slope			1	3	4	5	6	6	0.19
[4] Altitude				1	2	3	4	6	0.11
[5] Prox River					1	2	3	5	0.08
[6] Proxi Road						1	3	4	0.06
[7] LU/LC							1	3	0.04
[8] Aspect								1	0.02
•	3.23	4.09	6.12	11.25	16.03	22.58	29.33	39.00	1.00
$\lambda \; max = 8.661 \; CI = 0$	$0.094 \ CR = 0.067$								

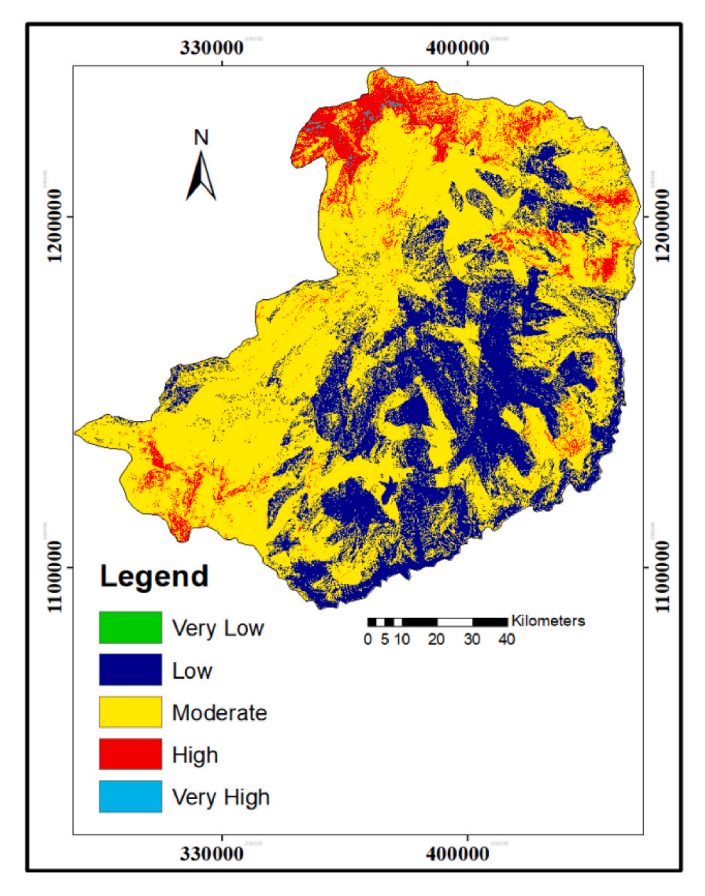


Fig. 16. LSM map produced using the AHP Method.

lowest, indicating that these parameters had the least significant influence on the occurrence of landslides. The weighted linear combination (WLC) method, one of the most widely used in multi-criteria decision approach evaluation, was used to combine all elements after the AHP pairwise comparison procedure (Ayalew et al., 2004).

The final step is calculating the consistency ratio (CR) to consider whether the judgment is relatively correct or not. If CR >0.1, our judgment is not accepted, and if it is less than 0.1, it is accepted according to (Saaty and engineering, 2004). The CR is calculated as follows: CR = CI (consistency index)/RI (random consistency index). CI  $= (\lambda \, max - n)/(n-1)$ , where  $\lambda \, max$  is the principal eigenvalue and n is the number of parameters employed in our case. Max is the value of each weight multiplied by the column total in our case (Table 2).

## 5. Discussion

In this study, a GIS-based MCDA, analytical hierarchy process model using selected landslide causative factors was used, and the resulting map is classified into four zones low, moderate, high, and very high classes. According to the produced landslide susceptibility maps and field observations, the highest frequencies of landslides were observed along the road corridors. This is due to the steepening of the road-cut slope, the weight of slope deposits during the rainy season, and roadcut dumps; this all leads to instability in the stable underlying support materials. As can be seen from the rainfall map of the study area, the area receives an average of 1401 mm/year of rainfall. This implies that, due to the fragile nature of the geological units in the area, sedimentary and basaltic units can aggravate the instability of slopes. Based on field observation of the study area, it was found that the slope materials that have experienced failures of varied forms are mainly; poorly graded colluvial, alluvial, and highly weathered materials located on the basaltic and sedimentary units. Most of the slope failures were associated with; high relative relief, steep slopes, heavy rainfalls, kinematic structural discontinuities, bare or sparsely vegetated lands, and stream bank and toe erosion.

The general finding of the study suggests that the most susceptible material for the occurrence of a landslide is highly weathered limestone, sandstone, and basalt. Most of the landslides were surficial and involved slope deposits, and colluvial material such as basalt, limestone, and sandstone. The hydrological conditions and human-made activities associated with gravitational movements favored by typical geological and geomorphological conditions cause a landslide. Generally, the result of this study can provide useful information for landslide management, academic institutions, and hazard mitigation organizations.

#### 6. Conclusions

This work focused on combining GIS and AHP methods to generate a landslide hazard zonation map in the East Gojjam Zone administrative area. The MCDM approach was used for hazard zonation mapping at East Gojjam Zone, which shows 0.11 % of the area covered by very high vulnerability, 7.34% of the area was high, 62.88 % of moderate, 29.66 % was low, and 0.00 % was very low-risk zones.

One of the most popular techniques and the first step in reducing the risk and hazards of landslides is vulnerability mapping. The results of the current study can be used by landslide mitigation planners, geohazard assessment offices, urban planners, and academic research institutions. As a result, there are some inherent limitations in the research that can be lessened by using a high-resolution data set, sophisticated data mining techniques, and taking into account temporal fluctuations in the dataset.

#### **Funding source**

This research did not receive any specific grant from funding agencies in the public, commercial, or not-for-profit sectors.

#### CRediT authorship contribution statement

Chalachew Tesfa: Conceptualization, Data curation, Formal analysis, Funding acquisition, Investigation, Methodology, Project administration, Resources, Software. Demeke Sewnet: Supervision, Validation, Visualization, Writing – original draft, Writing – review & editing.

## Declaration of competing interest

The authors declare that they have no known competing financial interests or personal relationships that could have appeared to influence the work reported in this paper.

#### Data availability

Data will be made available on request.

#### References

Addis, A., 2023. GIS– based flood susceptibility mapping using frequency ratio and information value models in upper Abay river basin, Ethiopia. Natural Hazards Research 3, 247–256.

Anbalagan, R., 1992. Landslide hazard evaluation and zonation mapping in mountainous terrain. Eng. Geol. 32, 269–277.

Arkar, S., Chandna, P., Pandit, K., Dahiya, N., 2023. An event-duration based rainfall threshold model for landslide prediction in Uttarkashi region, North-West Himalayas, India. Int. J. Earth Sci. 112, 1923–1939.

Asmare, D., Tesfa, C., 2022. Application and validation of the evaluation using slope stability susceptibility evaluation parameter rating system to debre werk area (Northwest Ethiopia). Geotech. Geol. Eng. 40, 2475–2488.

Asmare, D., Tesfa, C., Zewdie, M.M., 2023. A GIS-based landslide susceptibility assessment and mapping around the Aba Libanos area, Northwestern Ethiopia. Applied Geomatics 15, 265–280.

- Ayalew, L., Yamagishi, H., Ugawa, N., 2004. Landslide susceptibility mapping using GIS-based weighted linear combination, the case in Tsugawa area of Agano River, Niigata Prefecture, Japan. Landslides 1, 73–81.
- Corominas, J., Moya, J., 1999. Reconstructing recent landslide activity in relation to rainfall in the Llobregat River basin, Eastern Pyrenees, Spain. Geomorphology 30, 79–93.
- Crozier, M.J., Glade, T., 2005. Landslide hazard and risk: issues, concepts and approach. Landslide hazard and risk 1-40.
- Di Napoli, M., Di Martire, D., Bausilio, G., Calcaterra, D., Confuorto, P., Firpo, M., Pepe, G., Cevasco, A., 2021. Rainfall-induced shallow landslide detachment, transit and runout susceptibility mapping by integrating machine learning techniques and GIS-based approaches. Water 13, 488.
- Ermias, B., Raghuvanshi, T.K., Abebe, B., 2017. Landslide Hazard zonation (LHZ) around Alemketema town, north Showa zone, Central Ethiopia-a GIS based expert evaluation approach. Int. J. Earth Sci. Eng. 33–44.
- Guzzetti, F., Carrara, A., Cardinali, M., Reichenbach, P., 1999. Landslide hazard evaluation: a review of current techniques and their application in a multi-scale study, Central Italy. Geomorphology 31, 181–216.
- Guzzetti, F., Reichenbach, P., Cardinali, M., Galli, M., Ardizzone, F., 2005. Probabilistic landslide hazard assessment at the basin scale. Geomorphology 72, 272–299.
- Kazmin, V., Garland, C., 1973. Evidence of Precambrian block-faulting in the western margin of the Afar depression, Ethiopia. Geol. Mag. 110, 55–57.
- Kieffer, B., Arndt, N., Lapierre, H., Bastien, F., Bosch, D., Pecher, A., Yirgu, G., Ayalew, D., Weis, D., Jerram, D.A., 2004. Flood and shield basalts from Ethiopia: magmas from the African superswell. J. Petrol. 45, 793–834.
- Lang, A., Moya, J., Corominas, J., Schrott, L., Dikau, R., 1999. Classic and new dating methods for assessing the temporal occurrence of mass movements. Geomorphology 30, 33–52.
- Li, P., Wang, B., Chen, P., Zhang, Y., Zhao, S., 2023. Vulnerability assessment of the ecogeo-environment of mining cities in arid and semi-arid areas: a case study from Zhungeer, China. Ecol. Indicat. 152, 110364.
- Qazi, A., Singh, K., Vishwakarma, D.K., Abdo, H.G., 2023. GIS based landslide susceptibility zonation mapping using frequency ratio, information value and weight of evidence: a case study in Kinnaur District HP India. Bull. Eng. Geol. Environ. 82, 332
- Saaty, T.L., 2004. Decision making—the analytic hierarchy and network processes (AHP/ANP). J. Syst. Sci. Syst. Eng. 13, 1–35.

- Shano, L., Raghuvanshi, T.K., Meten, M., 2020. Landslide susceptibility evaluation and hazard zonation techniques—a review. Geoenvironmental Disasters 7, 1–19.
- Simane, B., Zaitchik, B.F., Ozdogan, M., 2013. Agroecosystem analysis of the Choke Mountain watersheds, Ethiopia. Sustainability 5, 592–616.
- Singh, A., Ashuli, A., Dhiman, N., Dubey, C.S., Shukla, D.P., 2023. Evaluating causative factors for landslide susceptibility along the Imphal-Jiribam railway corridor in the North-Eastern part of India using a GIS-based statistical approach. Environ. Sci. Pollut. Control Ser. 1–18.
- Soeters, R., Van Westen, C., 1996. Slope instability recognition, analysis and zonation. Landslides: investigation and mitigation 247, 129–177.
- Tadele, T., 2022. Landslide Hazard Assessment and Zonation by Using Slope Susceptibility Evaluation Parameter (SSEP) Rating Scheme-A Case from DebreSina, Northern Ethiopia.
- Tefera, M., Chernet, T., Haro, W., 1996. Geology of Ethiopia. Geological Survey of Ethiopia.
- Tesfa, C., 2022. GIS-based AHP and FR methods for landslide susceptibility mapping in the Abay gorge, dejen–renaissance bridge, central, Ethiopia. Geotech. Geol. Eng. 40, 5029–5043.
- Tesfa, C., Woldearegay, K., 2021. Characteristics and susceptibility zonation of landslides in Wabe Shebelle Gorge, south eastern Ethiopia. J. Afr. Earth Sci. 182, 104275.
- Van Westen, C.J., Piya, B.K., Guragain, J., 2005. Geo-information for Urban Risk Assessment in Developing Countries: the SLARIM Project. *Geo-Information for Disaster Management*. Springer.
- Van Westen, C., Van Asch, T.W., Soeters, R., 2006. Landslide hazard and risk zonation—why is it still so difficult? Bull. Eng. Geol. Environ. 65, 167–184.
- Vishwakarma, A., Goswami, A., Pradhan, B., 2021. Prioritization of sites for Managed Aquifer Recharge in a semi-arid environment in western India using GIS-Based multicriteria evaluation strategy. Groundwater for sustainable development 12, 100501
- Woldearegay, K., 2013. Review of the occurrences and influencing factors of landslides in the highlands of Ethiopia: with implications for infrastructural development. Momona Ethiopian Journal of Science 5, 3–31.
- Yang, Z., Lu, H., Zhang, Z., Liu, C., Nie, R., Zhang, W., Fan, G., Chen, C., Ma, L., Dai, X., 2023. Visualization analysis of rainfall-induced landslides hazards based on remote sensing and geographic information system-an overview. International Journal of Digital Earth 16, 2374–2402.
- Zewdie, M.M., Tesfa, C., 2023. GIS-based MCDM modeling for suitable dam site identification at Yeda watershed, Ethiopia. Arabian J. Geosci. 16, 369.